A Water Soluble Pd_2L_4 Cage for Selective Binding of Neu5Ac

Xander Schaapkens,[a] Roy N. van Sluis,[a] Eduard O. Bobylev,[a] Joost N. H. Reek,[a] and Tiddo J. Mooibroek*[a]

Abstract: The sialic acid *N*-acetylneuraminic acid (Neu5Ac) and its derivatives are involved in many biological processes including cell-cell recognition and infection by influenza. Molecules that can recognize Neu5Ac might thus be exploited to intervene in or monitor such events. A key obstacle in this development is the sparse availability of easily prepared molecules that bind to this carbohydrate in its natural solvent; water. Here, we report that the carbohydrate binding pocket of an organic soluble $[Pd_2L_4]^{4+}$ cage could be equipped with guanidinium-terminating dendrons to give the water soluble $[Pd_2L_4][NO_3]_{16}$ cage **7**. It was shown by means of NMR spectroscopy that **7** binds selectively to anionic monosaccharides and strongest to Neu5Ac with $K_a = 24\ M^{-1}$. The cage had low to no affinity for the thirteen neutral saccharides studied. Aided by molecular modeling, the selectivity for anionic carbohydrates such as Neu5Ac could be rationalized by the presence of charge assisted hydrogen bonds and/or the presence of a salt bridge with a guanidinium solubilizing arm of **7**. Establishing that a simple coordination cage such as **7** can already selectively bind to Neu5Ac in water paves the way to improve the stability, affinity and/or selectivity properties of M_2L_4 cages for carbohydrates and other small molecules.

Introduction

Sialic acids, a class of α-keto acid sugars, have been found on the distal ends of cell surface glycoconjugates and play a wide variety of biological roles, especially in cell-to-cell recognition.[1] The most common member is *N*-acetylneuraminic acid (Neu5Ac), which is utilized by influenza or other viruses to enter mammalian cells.[2] Neu5Ac is also found at the end of tetrasaccharide Sialyl Lewis^X **1** (sLe^x, Figure 1a) and clinical studies showed the importance of sLe^x in leukocyte adhesion deficiency,[3] inflammatory response,[4] (in vitro) fertilization,[5] coronavirus binding,[6] and cancer metastasis.[7] An example is the study of molecular sensors for sLe^x, which facilitates extravasation of cancer cells out of the blood stream (metastasis), displaying leukocyte mimicry.[8] While Neu5Ac is typically O-linked to other molecules as α-anomer (axial carboxylate),[1]

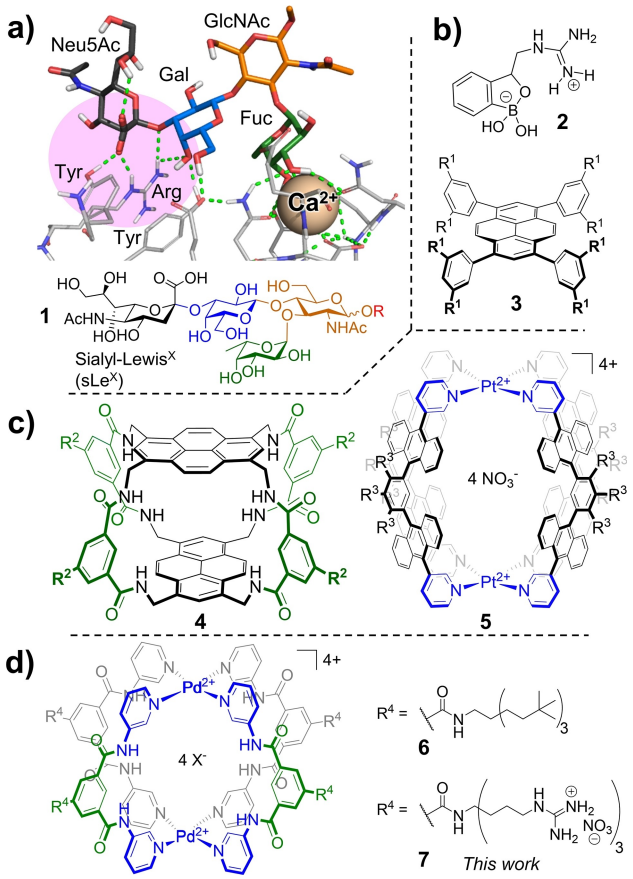

Figure 1. a) Sialyl Lewis^X **1** (sLe^x) bound to the E-selectin binding site as found in PDB entry 1G1T with charge assisted HBs highlighted in magenta.[11] b) Two artificial carbohydrate receptors that bind to Neu5Ac in part due to charge assisted HBs.[12] R^1 = guanindinium terminating dendron. c) Left: macrocycle **4** selective for GlcNAc-β-OMe. R^2 = carboxylate terminating dendrimer.[13] Right: Pt_2L_4 cage **5** selective for disaccharides where L = anthracene functionalized dipyridyl ligand and R^3=O$(CH_2)_2$OMe.[14] d) Pd_2L_4 cages **6** (X=BF_4^-)[15] and **7** (X=NO_3^-) where L = isophthalamide linked dipyridyl ligand and R^4 a solubilizing group.

[a] *X. Schaapkens, R. N. van Sluis, E. O. Bobylev, Prof. Dr. J. N. H. Reek, Dr. T. J. Mooibroek*
Van 't Hoff Institute for Molecular Sciences
University of Amsterdam
Science Park 904, 1098 XH, Amsterdam (The Netherlands)
E-mail: t.j.mooibroek@uva.nl

Supporting information for this article is available on the WWW under https://doi.org/10.1002/chem.202102176

the chemical antecedent to such linkages is cytidine-5′-monophospho-β-Neu5Ac.[1,9] Unlinked Neu5Ac is predominantly present as the β-anomer in solution and has a rich *in vivo* chemistry.[1,10] Molecules that can bind selectively to Neu5Ac and its derivatives might thus be exploited to understand, monitor or intervene in a range of biological processes.

Inspiration for the development of Neu5Ac binders can be drawn from selectins, a subclass of lectins (carbohydrate binding proteins). As is illustrated in Figure 1a for crystal structure 1G1T (human E-selectin), there is a high degree of interaction complementarity in the binding mode with sLe^x.[11] Notably, the anionic Neu5Ac fragment of sLe^x forms a salt-bridge with an arginine residue and the galactose fragment has strong charge assisted hydrogen bonds (HBs) with the same arginine residue (highlighted in magenta).

The beneficial effect of employing charge assisted HBs to bind sialic acid derivatives has been mimicked by the artificial receptors **2**[12a] and **3**[12b] shown in Figure 1b. The benzoboroxole-based receptor **2** can bind covalently to Neu5Ac with its borane part and binding is further enhanced by the presence of the nearby guanidinium group.[12a] Pyrenyl platform **3** was intended to bind carbohydrates in water using CH···π interactions and showed enhanced affinity for Neu5Ac when equipped with guanidinium-terminating dendrons (R^1).[12b] Another binding strategy is the use of covalent macrocyclic compounds that can encapsulate a carbohydrate in aqueous media.[13,16]

For example, macrocycle **4** (Figure 1c, left)[13] is highly selective for GlcNAc-β-OMe ($K_a \approx 18{,}000\ M^{-1}$ in water) by encapsulating the carbohydrate by regular HBs and CH···π interactions.[17] However, such covalent macrocycles are not selective for Neu5Ac or related anionic carbohydrates.[16c–e] This can be rationalized by the presence of anionic dendrimers (R^2) used to solubilize the hydrophobic binding pockets.

Contrarily, coordination cages based on a dipyridyl ligand (L) an a square planar d^8 metal (M, for example Pd^{2+} or Pt^{2+}) are positively charged and are known to have affinity for anionic guests.[18] Another advantage of such coordination cages is the reversibility of the pyridine-metal bond. This allows for non-productive oligomerization products to become intermediates towards the desired macrocycle, thus evading low-yielding macrocyclization reactions needed in the synthesis of covalent cages. Recently, two examples of coordination cages with the structure $[M_2L_4]^{4+}$ have been reported with affinity for carbohydrates.[14–15] As is exemplified in Figure 1c (right), $[Pt_2L_4]^{4+}$ cage **5** is based on dipyridyl ligands separated by anthracene moieties. This cage bound selectively to D-sucrose ($K_a \approx 1{,}000\ M^{-1}$) by virtue of shape-complementarity and multiple CH···π interactions between the carbohydrate and the polyaromatic cavity of **5**.[14] A similar $[M_2L_4]^{4+}$ cage was reported (**6** in Figure 1d) where the dipyridyl ligands are separated by isophtalamides, similar to macrocycle **4**.[15] Cage **6** had an organic solubility handle and could be studied in CD_2Cl_2 containing 10% DMSO-d_6, where selectivity towards *n*-octyl-β-glucoside ($K_a \approx 51\ M^{-1}$) *versus* *n*-octyl-β-galactoside ($K_a \approx 29\ M^{-1}$) was observed.

We thus wondered what the binding properties of a cage such as **6** would be in aqueous solution, in particular for anionic carbohydrates like Neu5Ac. To this end, the solubility handles of the ligands in **6** were replaced by guanidinium-terminating dendrons to make the $[Pd_2L_4]^{16+}$ cage **7** (Figure 1d). Herein, we report that **7** has selective affinity for anionic sugars, particularly for Neu5Ac, and that **7** has very low to no affinity for common neutral mono- and disaccharides.

Results and Discussion

The synthesis of the ligand precursor to cage **7** (penta nitric acid salt **13**) is shown in Scheme 1. The starting trimesic pentafluorophenyl (PFP) ester **8** and amine **9** were synthesized according to literature procedures[19] and then coupled to each other to form bis-PFP ester **10** in 62% yield by using a previously reported protocol.[15,19d] Subsequently, the remaining PFP esters of **10** were substituted by 3-aminopyridine to afford **11**.[15] Deprotection of the Boc groups of **11** followed by basification and treatment with bis-boc-pyrazolocarboxamidine afforded hexa-boc guanidine **12** in 69% yield.[20] The desired guanidinium ligand **13** could be obtained in 74% yield after treatment of **12** with 1 M nitric acid in a water/1,4-dioxane solvent mixture. The pyridyl rings in **13** could be selectively deprotonated by the addition of two equivalents of sodium hydroxide. The subsequent addition of a $Pd(NO_3)_2$ solution (0.55 eq.) gave cage **7** in a quantitative yield based on ^{1}H NMR. [Note: As is detailed in Section S2 of the Supporting

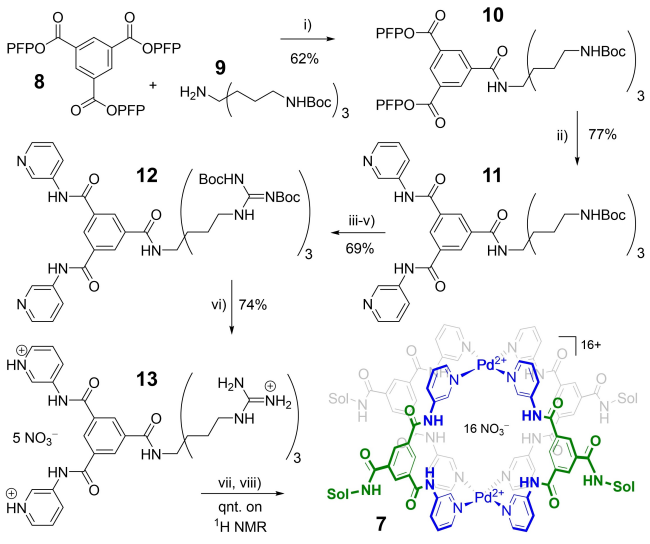

Scheme 1. Synthesis of cage **7** from ligand **13**, prepared from previously reported building blocks following (adjusted) literature protocols.[15,19–20] PFP = pentafluorophenyl, Boc = *tert*-Butyloxycarbonyl, Sol = guanidinium solubilizing group. Conditions: i) *N*,*N*-diisopropylethylamine, 42 h at room temperature (RT) in tetrahydrofuran; ii) 6 eq. 3-aminopyridine, 41 h at 100 °C in pyridine; iii) 4 h at RT in 4 M HCl in dioxane/water; iv) neutralization with NaOH and basification with NEt_3; v) 6 eq. bis-Boc-pyrazolocarboxamide, 20 h at RT (with dichloromethane); vi) 1 M HNO_3, 22 h at 50 °C in dioxane/water; vii) 2 eq. NaOH in D_2O;viii) 0.55 eq. $Pd(NO_3)_2$ in D_2O (see also Figure 2). See Section S2 for experimental details and full characterizations.

Information, an alternative route to prepare ligand **13** was unproductive due to reaction compatibility issues between PFP-esters and the Boc-linked NH of diBoc-protected guanidines.]

The synthesis of **7** from **13** could also be followed in D_2O by ^1H NMR, as shown by the stacked spectra in Figure 2a (top). Upon addition of 2 equivalents of NaOH the resonances belonging to the pyridyl ring in **13** were found significantly upfield, which is in line with deprotonation of the pyridyl nitrogens.

Subsequent stepwise addition of $Pd(NO_3)_2$ resulted in the disappearance of dipyridyl ligand signals with the proportional appearance of a new set of resonances.

The emerging Pd-complex and its parent ligand thus appear to be in slow exchange relative to the NMR time scale. All proton resonances of the resulting well-defined spectrum could be identified and are consistent with that of cage **7**. In particular the large downfield shifts of proton resonances such as **a** (8.41→8.86) and **d** (8.77→9.74) are indicative of pyridyl-palladium coordination.[21]

The 2D DOSY NMR of this sample reveals that the diffusion constant (*D*) of **7** (log(*D*) = −9.83) is substantially larger than that of the neutralized ligand (log(*D*) = −9.57) which is also consistent with cage formation (see bottom of Figure 2a). Furthermore, the isotope distribution of a species with largest monoisotopic mass *m/z* = 476.1798 (Figure 2b) measured with CSI HRMS is in agreement with a simulated distribution of $[\mathbf{7}(NO_3)_3Cl_6]^{7+}$ with largest monoisotopic mass of *m/z* = 476.1823. The modelled molecular formula of $[\mathbf{7}(NO_3)_3Cl_6]^{7+}$ includes some deuterium and Cl^- because the solution was measured from a D_2O sample in undeuterated solvent containing trace amounts of salts (see Supporting Information and Figures S74–S90 for details).

With the water soluble $[Pd_2L_4]^{16+}$ cage **7** in hand, the binding affinity for the carbohydrates listed in Table 1 was investigated by ^1H NMR titration experiments in D_2O. Titrations with charge neutral carbohydrates **14**–**26** to about 140 mM only resulted in minor near-linear peaks shifts of some resonances of **7** with $\Delta\delta^{max} \approx 0.02$ p.p.m. on average (see Figures S92–S104). These shifts could not result from the dilution of **7**, as a dilution study in the concentration range used during titrations revealed that all resonances remained stationary (see Figure S91). Attempts to fit these shifts to a binding model was not feasible and could only be roughly modelled (not fitted) to binding with an affinity around or below the detection limit of ~3 M^{-1}. We thus interpret these shifts as resulting from very weak binding of ≤ 3 M^{-1} (entry 1, Table 1), spanning only the very start of possible binding curves.

Addition of neutralized solutions of **27**–**29**, did result in significant non-linear shifting of the resonances of **7**, with clear sings of saturation (Figures S105–S107). These shifts could be fitted accurately to a 1:1 binding model resulting in the binding constants listed in entries 2–4 of Table 1.

Selected spectra of the titration with **29** are shown in Figure 3a. With increasing concentration of Neu5Ac **29**, aro-

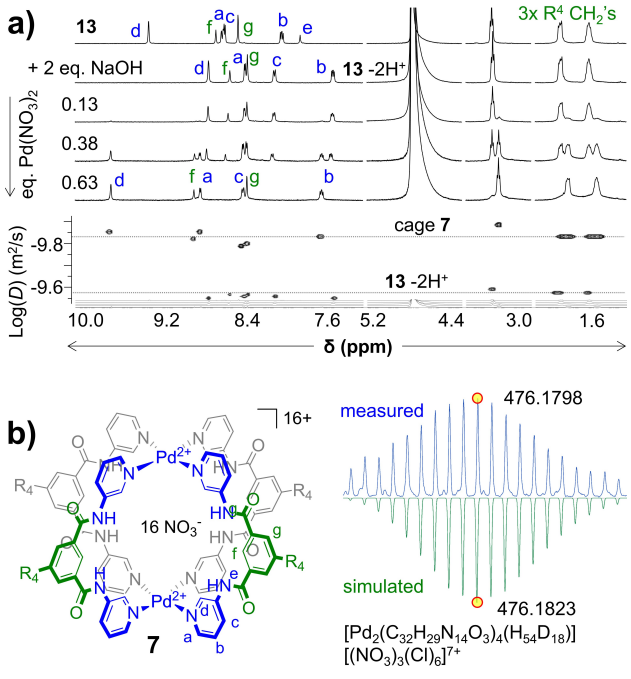

Figure 2. a) Top: stepwise formation of **7** by deprotonation of the pyridyls in **13** (top two spectra) followed by stepwise addition of $Pd(NO_3)_2$ as a 10 mM solution. Bottom: overlay of the 2D DOSY NMR spectra of **7** and **13** with deprotonated pyridyl rings. b) representation of **7** with labelled protons and CSI HRMS isotope distribution with indicated highest isotopic mass as measured from a D_2O solution (top, blue) and simulated (bottom, green).

Table 1. Overview of binding studies performed with **7** and the structures of titrants **14**–**29**.

Entry	Guest	K_a (M^{-1})[a]	Correlation of fit (r^2)[b]
1	**14**–**26**	≤3	–
2	**27**	6.6 ± 0.2	0.9974
3	**28**	8.3 ± 0.3	0.9609
4	**29**	24.0 ± 0.2	0.9981

[a] Obtained by curve fitting ^1H NMR resonance shifts using HypNMR;[22] [b] Correlation of fit computed over all fitted data points.

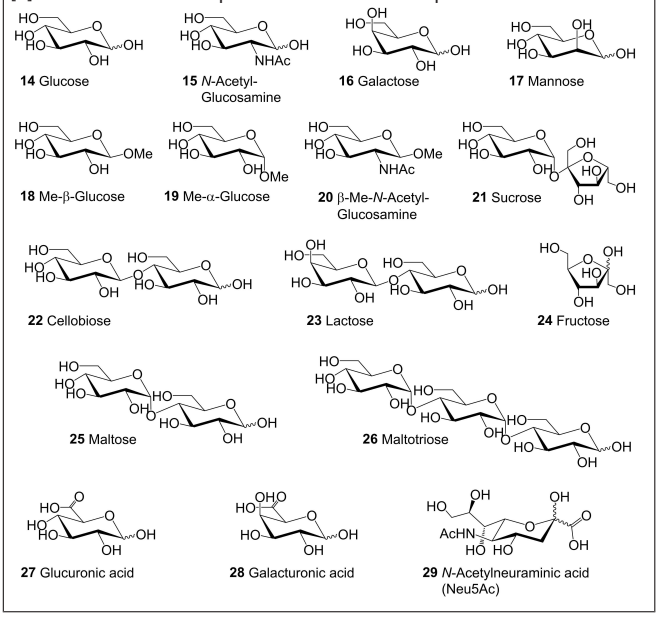

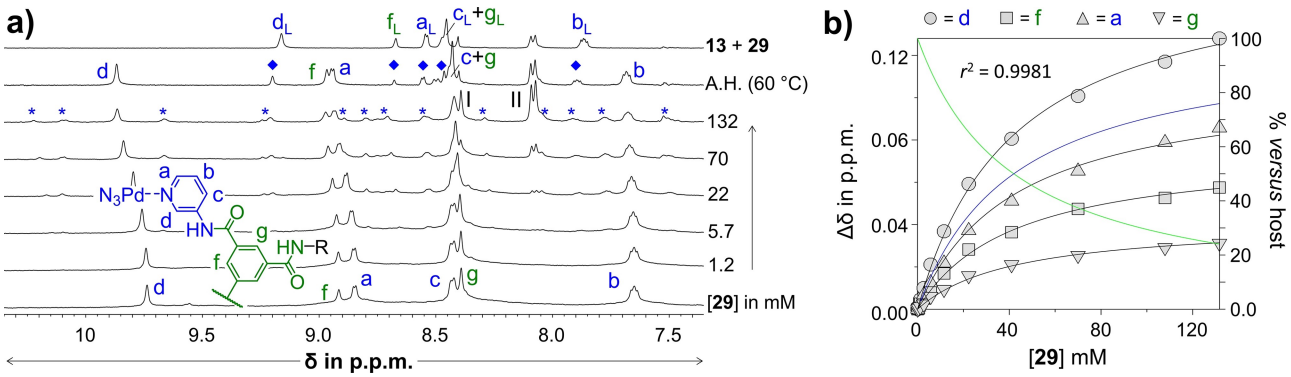

Figure 3. a) Partial ^{1}H NMR spectra of **7** titrated with Neu5Ac **29** in D_2O, a spectrum at the end of the titration after heating ('A. H.') at 60 °C, and a spectrum of **13** + **29** at the same concentration as at the end of the titration. Assignment of the proton signals: [**7**·**29**] major symmetric species (a-g), asymmetric species (*), [**13**·**29**] minor symmetrical species (a_L–g_L), and a small impurity present in **29** (I and II) that does not bind (see Figure S108); b) HypNMR fit (black lines) using a 1:1 binding model to the shifting of indicated resonances (grey symbols) of the symmetrical signals of **7** to give $K_a = 24.0 \pm 0.2$ M^{-1} with indicated goodness of for (r^2). The speciation is also shown as unbound **7** (host, green line) and the [**7**·**29**] adduct (blue line).

matic signals **a**, **b**, **d**, **f** and **g** shifted downfield and broadened slightly. In the presence of a large excess of **29**, a minor species with lower symmetry arose, marked with blue asterisks in Figure 3a. This species disappeared after heating at 60 °C ('A.H.'), while the major species of [**7**·**29**] persisted and another minor symmetrical species appeared (marked with diamonds). This new set of resonances was nearly identical to a solution of deprotonated ligand **13** and neutralized **29** at the same concentration as present in the titration (shown at the top of Figure 3a and assigned with subscript 'L'). The minor symmetrical species (diamonds) present after heating is thus probably ligand bound to **29**, with the ligand originating from cage decomposition (likely driven by Pd-plating). To quantify binding of the major symmetrical species **7**, the peak shifting could be fitted to a 1:1 model using HypNMR[22] as shown in Figure 3b. This fitting gave the association constant (K_a) of 24.0 ± 0.2 M^{-1} listed in entry 4 of Table 1 with an excellent goodness of fit of $r^2 = 0.9981$.

To further understand binding of **7** with **29**, selective 1D nuclear Overhauser effect (nOe) NMR spectra were recorded after heating at 60 °C, as shown in Figure 4b. For reference purposes, the ^{1}H NMR spectrum of **29** is shown in Figure 4a together with an assignment that is based on a full structure elucidation of **29** (see Section S3 for full details). As is shown in Figure 4b, clear nOe signals were observed between irradiated cage protons **d**, **f**/**a** and **c**/**g** and carbohydrate protons **c3**, **c9** and **c11**. Proton **d** of **7** also shifted the most when binding to **29** (see Figure 3). The much weaker nOe with proton **b** suggest that these are further away from the C–H protons of Neu5Ac **29**. It is worth pointing out that protons **c3**, **c9**, and **c11** are located on different sides of **29** and that **c3** and **c9** are even opposite to each other (see Figure 4a). The fact that nOe's were observed to these signals thus implies that **29** is bound inside **7**.

The titration data (Table 1) clearly show that **7** is selective for anionic monosaccharides, in particular for Neu5Ac **29**, and that **7** binds about equally well to glucoronate **27** and galacturonate **28**. To rationalize these observations, some

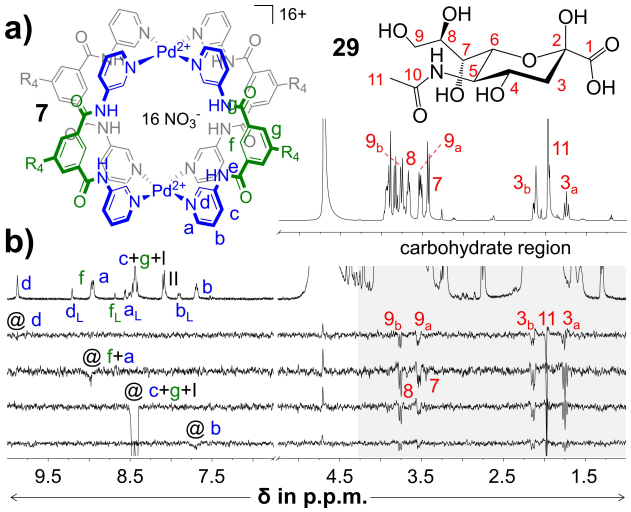

Figure 4. a) structures of **7** and β-Neu5Ac **29** with reference ^{1}H NMR spectrum. Assignment of **29** in main text is with a '**c**' for 'carbohydrate' in front of the number to distinguish it from other assignments. b) 1D selective NOESY spectrum of [**7**·**29**]$^{15+}$ with $t_m = 500$ ms after heating at 60 °C. See section S3 for full structural elucidation of β-Neu5Ac **29**.

molecular models were generated of cage **7** bound to the β-anomers of anionic carbohydrates **27**, **28** and **29** using density functional theory (DFT, see Section S4 for details).

Shown in the top of Figure 5a is the space filling representation of a model of **7** that fully encapsulates glucoronate **27**, with **OH-3** protruding from one of the portals. Interestingly, as is shown in the bottom of Figure 5a, **OH-3** is not involved in a HB to an amide, while all the other hydroxyl groups are. Rather, **OH-3** is involved in the only (and weak) charge assisted HB involving the pyridyl C–H (blue arrow). The carboxylate is furthermore held in place by four amidic HBs with H···O distances in the range of 2.0–2.3 Å. This four-pronged charge assisted HB interaction might rationalize the selectivity of **7** for the anionic glucoronate **27** over the neutral glucose **14**. The model of **7** with galacturonate **28** is very similar

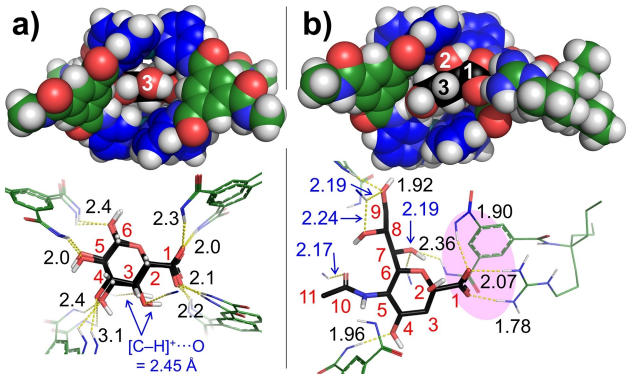

Figure 5. Models of **7** bound to anionic carbohydrates calculated by DFT/ωB97X–D/6–31G*. a) top: space filling representation of **7** bound to **27**; bottom: hydrogen bonding pattern of the [**7**·**27**] model overlaid with the [**7**·**28**] model. The C-atoms of **27** and **28** are labelled in red and the distances (in Å) are averages for both models. See Figure S116 for more details; b) top: space filling model of Neu5Ac **29** bound to a model of **7** with a guanidinium arm incorporated; bottom: hydrogen bonding pattern of [**7**·**29**] with distances in Å and C-atoms of **29** labelled in red. The structure is similar to a structure without such a guanidiunium arm, see Figure S117.

to the [**7**·**27**] model, which is evident from the overlaid HB patterning at the bottom of Figure 5a (see also Figure S116). Here too the carboxylate is held in place by four amidic HBs and **OH-3** is the only hydroxyl that has no HB to an amide and only weakly to a pyridyl C–H (blue arrow). This absence of an amidic HB with **OH-3** in both **27** and **28** might explain the lack in selectivity observed between these two carbohydrates. As can be seen in the top of Figure 5b, modelling the binding of **7** to Neu5Ac **29** resulted in a complex where the anomeric center (**C2**) protrudes through one of the four portals of **7**. The glyceryl (**C7**–**C9**) and acetyl (**C10**, **C11**) fragments point out of two other portals (see Figure S117 for details). Presumably, the carboxylate and hydroxyl group on **C2** of **29** are too large to be accommodated in the interior of **7** in the same manner as modelled for the carboxylates in **27** and **28** (Figure 5a). Moreover, the guanidinium arm that was incorporated in this model of **7** formed a strong salt-bridge with the carboxylate of **29**. This is particularly evident from the HB pattern in the [**7**·**29**] model shown in the bottom of Figure 5b. Highlighted in magenta are the three strong charge assisted HBs with H···O distances in the range of 1.8–2.1 Å, which resemble the charge assisted HBs found in PDB entry 1G1T (Figure 1a).[11] Additionally, there are three amidic HBs and four relatively strong HBs involving pyridyl C–H's with H···O≈2.2 Å (blue arrows). The salt-bridge formation, together with the encapsulation of **29** via three of the four portals of **7**, the three amidic HBs and the four HBs with pyridyl C–H's observed in the model can offer a rationale for the ~3–4 fold selectivity observed for **29** over **27**/**28** (see Table 1).

Conclusions

A previous reported $[Pd_2L_4]^{4+}$ cage was rendered water soluble by introducing guanidinium solubility groups on the ligand to form the $[Pd_2L_4]^{16+}$ cage **7**. Titrations of **7** with common carbohydrates revealed selectivity for anionic carbohydrates. While the binding affinities towards neutral mono- and disaccharides was near or under the detection limit of K_a ≈3 M^{-1}, the binding affinities for anionic carbohydrates **27**, **28** and **29** were found to be 6.6, 8.3 and 24 M^{-1}, respectively. Cage **7** is thus at least 8 times more selective for **29** than for neutral saccharides. This selectivity could be rationalized based on DFT modelling and likely originates from complementary ion-pair formation between the anionic sugars and cationic **7** by various (charge assisted) HBs, much like those found in nature.

The selectivity for anionic carbohydrates in aqueous solution is rare,[12a] and has not yet been reported with similar isophthalamide macrocyclic structures held together by either covalent[13,16a–k] or coordination[15] bonds. While the affinities found are on the lower end, this study establishes the principle that a coordination cage such as **7** can selectively bind to anionic carbohydrates in water. This finding thus paves the way for further improvements of coordination cages to enhance their stability, affinity and/or selectivity properties. Ultimately, such developments could lead to selective synthetic lectins for Neu5Ac and its α/β-derivatives that can be used in biological studies such as Western blotting, targeted drug delivery.

Acknowledgements

This research was financially supported by the Netherlands Organization for Scientific Research (NWO) with VIDI grant number 723.015.006.

Conflict of Interest

There are no conflicts to declare.

Keywords: carbohydrate recognition · host-guest systems · molecular recognition · sialic acids · self-assembly

[1] T. Angata, A. Varki, *Chem. Rev.* **2002**, *102*, 439–469.
[2] S. X. Tong, X. Y. Zhu, Y. Li, M. Shi, J. Zhang, M. Bourgeois, H. Yang, X. F. Chen, S. Recuenco, J. Gomez, *PLoS Pathog.* **2013**, *9*, Art. Nr.: e1003657.
[3] S. Hanna, A. Etzioni, N. Y. A. S. Annals, *Ann. N. Y. Acad. Sci.* **2012**, *1250*, 50–55.
[4] a) M. Fukuda, N. Hiraoka, J. C. Yeh, *J. Cell Biol.* **1999**, *147*, 467–470; b) S. R. Barthel, J. D. Gavino, L. Descheny, C. J. Dimitroff, *Expert Opin. Ther. Targets* **2007**, *11*, 1473–1491.
[5] P. C. Pang, P. C. N. Chiu, C. L. Lee, L. Y. Chang, M. Panico, H. R. Morris, S. M. Haslam, K. H. Khoo, G. F. Clark, W. S. B. Yeung, *Science* **2011**, *333*, 1761–1764.
[6] a) M. A. Tortorici, A. C. Walls, Y. F. Lang, C. Y. Wang, Z. S. Li, D. Koerhuis, G. J. Boons, B. J. Bosch, F. A. Rey, R. J. de Groot, *Nat. Struct. Mol. Biol.* **2019**, *26*, 481–489; b) W. T. Li, R. J. G. Hulswit, I. Widjaja, V. S. Raj, R. McBride, W. J. Peng, W. Widagdo, M. A. Tortorici, B. van Dieren, Y. Lang, *Proc. Natl. Acad. Sci. USA* **2017**, *114*, E8508–E8517.
[7] a) F. Q. Jin, F. S. Wang, *Glycoconjugate J.* **2020**, *37*, 277–291; b) S. S. Li, C. K. M. Ip, M. Y. H. Tang, M. K. S. Tang, Y. Tong, J. W. Zhang, A. A. Hassan, A. S. C. Mak, S. Yung, T. M. Chan, *Nat. Commun.* **2019**, *10*, Art. Nr.: 2406; c) S. Julien, A. Ivetic, A. Grigoriadis, D. Qize, B. Burford, D. Sproviero, G. Picco, C. Gillett, S. L. Papp, L. Schaffer, *Cancer Res.* **2011**, *71*, 7683–7693; d) H. Läubli, L. Borsig, *Semin. Cancer Biol.* **2010**, *20*, 169–

177; e) C. Ohyama, S. Tsuboi, M. Fukuda, *EMBO J.* **1999**, *18*, 1516–1525; f) R. Kannagi, M. Izawa, T. Koike, K. Miyazaki, N. Kimura, *Cancer Sci.* **2004**, *95*, 377–384.

[8] a) G. Kaur, H. Fang, X. M. Gao, H. B. Li, B. H. Wang, *Tetrahedron* **2006**, *62*, 2583–2589; b) W. Q. Yang, H. Y. Fan, X. M. Gao, S. H. Gao, V. V. R. Karnati, W. J. Ni, W. B. Hooks, J. Carson, B. Weston, B. H. Wang, *Chem. Biol.* **2004**, *11*, 439–448; c) W. Q. Yang, S. H. Gao, X. M. Gao, V. V. R. Karnati, W. J. Ni, B. H. Wang, W. B. Hooks, J. Carson, B. Weston, *Bioorg. Med. Chem. Lett.* **2002**, *12*, 2175–2177; d) G. S. Jacob, C. Kirmaier, S. Z. Abbas, S. C. Howard, C. N. Steininger, J. K. Welply, P. Scudder, *Biochemistry* **1995**, *34*, 1210–1217.

[9] a) F. Amann, C. Schaub, B. Muller, R. R. Schmidt, *Chem. Eur. J.* **1998**, *4*, 1106–1115; b) M. Gilbert, R. Bayer, A. M. Cunningham, S. Defrees, Y. H. Gao, D. C. Watson, N. M. Young, W. W. Wakarchuk, *Nat. Biotechnol.* **1998**, *16*, 769–772; c) D. N. Kwon, K. H. Lee, M. J. Kang, Y. J. Choi, C. Park, J. J. Whyte, A. N. Brown, J. H. Kim, M. Samuel, J. D. Mao, *Sci. Rep.* **2013**, *3*, Art. Nr.: 01981.

[10] a) I. C. Blomfield, *Microbiol. Spectr.* **2015**, *3*, Art. Nr.: MBP-0015–2014; b) A. Bell, E. Severi, M. Lee, S. Monaco, D. Latousakis, J. Angulo, G. H. Thomas, J. H. Naismith, N. Juge, *J. Biol. Chem.* **2020**, *295*, 13724–13736.

[11] W. S. Somers, J. Tang, G. D. Shaw, R. T. Camphausen, *Cell* **2000**, *103*, 467–479.

[12] a) A. Di Pasquale, S. Tommasone, L. L. Xu, J. Ma, P. M. Mendes, *J. Org. Chem.* **2020**, *85*, 8330–8338; b) T. S. Carter, T. J. Mooibroek, P. F. N. Stewart, M. P. Crump, M. C. Galan, A. P. Davis, *Angew. Chem. Int. Ed.* **2016**, *55*, 9311–9315; *Angew. Chem.* **2016**, *128*, 9457–9461.

[13] P. Rios, T. S. Carter, T. J. Mooibroek, M. P. Crump, M. Lisbjerg, M. Pittelkow, N. T. Supekar, G. J. Boons, A. P. Davis, *Angew. Chem. Int. Ed.* **2016**, *55*, 3387–3392; *Angew. Chem.* **2016**, *128*, 3448–3453.

[14] M. Yamashina, M. Akita, T. Hasegawa, S. Hayashi, M. Yoshizawa, *Sci. Adv.* **2017**, *3*, Art. Nr.: e1701126.

[15] X. Schaapkens, E. O. Bobylev, J. N. H. Reek, T. J. Mooibroek, *Org. Biomol. Chem.* **2020**, *18*, 4734–4738.

[16] a) A. P. Davis, *Chem. Soc. Rev.* **2020**, *49*, 2531–2545; b) O. Francesconi, S. Roelens, *ChemBioChem* **2019**, *20*, 1329–1346; c) Y. Ferrand, E. Klein, N. P. Barwell, M. P. Crump, J. Jimenez-Barbero, C. Vicent, G. J. Boons, S. Ingale, A. P. Davis, *Angew. Chem. Int. Ed.* **2009**, *48*, 1775–1779; *Angew. Chem.* **2009**, *121*, 1807–1811; d) J. D. Howgego, C. P. Butts, M. P. Crump, A. P. Davis, *Chem. Commun. (Camb.)* **2013**, *49*, 3110–3112; e) P. Stewart, C. M. Renney, T. J. Mooibroek, S. Ferheen, A. P. Davis, *Chem. Commun. (Camb.)* **2018**, *54*, 8649–8652; f) R. A. Tromans, T. S. Carter, L. Chabanne, M. P. Crump, H. Y. Li, J. V. Matlock, M. G. Orchard, A. P. Davis, *Nat. Chem.* **2019**, *11*, 52–56; g) N. Chandramouli, Y. Ferrand, G. Lautrette, B. Kauffmann, C. D. Mackereth, M. Laguerre, D. Dubreuil, I. Huc, *Nat. Chem.* **2015**, *7*, 334–341; h) P. Mateus, B. Wicher, Y. Ferrand, I. Huc, *Chem. Commun. (Camb.)* **2018**, *54*, 5078–5081; i) O. Francesconi, F. Cicero, C. Nativi, S. Roelens, *ChemPhysChem* **2020**, *21*, 257–262; j) O. Francesconi, M. Martinucci, L. Badii, C. Nativi, S. Roelens, *Chem. Eur. J.* **2018**, *24*, 6828–6836; k) T. J. Mooibroek, M. P. Crump, A. P. Davis, *Org. Biomol. Chem.* **2016**, *14*, 1930–1933; l) P. Rios, T. J. Mooibroek, T. S. Carter, C. Williams, M. R. Wilson, M. P. Crump, A. P. Davis, *Chem. Sci.* **2017**, *8*, 4056–4061.

[17] K. L. Hudson, G. J. Bartlett, R. C. Diehl, J. Agirre, T. Gallagher, L. L. Kiessling, D. N. Woolfson, *J. Am. Chem. Soc.* **2015**, *137*, 15152–15160.

[18] a) H. Dasary, R. Jagan, D. K. Chand, *Inorg. Chem.* **2018**, *57*, 12222–12231; b) S. Yi, V. Brega, B. Captain, A. E. Kaifer, *Chem. Commun. (Camb.)* **2012**, *48*, 10295–10297; c) D. W. Zhang, T. K. Ronson, J. Mosquera, A. Martinez, J. R. Nitschke, *Angew. Chem. Int. Ed.* **2018**, *57*, 3717–3721; *Angew. Chem.* **2018**, *130*, 3779–3783; d) R. Custelcean, P. V. Bonnesen, N. C. Duncan, X. H. Zhang, L. A. Watson, G. Van Berkel, W. B. Parson, B. P. Hay, *J. Am. Chem. Soc.* **2012**, *134*, 8525–8534; e) Q. Q. Wang, S. Gonell, S. Leenders, M. Durr, I. Ivanovic-Burmazovic, J. N. H. Reek, *Nat. Chem.* **2016**, *8*, 225–230.

[19] a) H. A. Bruson, T. W. Riener, *J. Am. Chem. Soc.* **1943**, *65*, 23–27; b) G. R. Newkome, C. N. Moorefield, K. J. Theriot, *J. Org. Chem.* **1988**, *53*, 5552–5554; c) C. Ji, P. A. Miller, M. J. Miller, *J. Am. Chem. Soc.* **2012**, *134*, 9898–9901; d) H. Destecroix, C. M. Renney, T. J. Mooibroek, T. S. Carter, P. F. N. Stewart, M. P. Crump, A. P. Davis, *Angew. Chem. Int. Ed.* **2015**, *54*, 2057–2061; *Angew. Chem.* **2015**, *127*, 2085–2089.

[20] a) A. Unciti-Broceta, E. Holder, L. J. Jones, B. Stevenson, A. R. Turner, D. J. Porteous, A. C. Boyd, M. Bradley, *J. Med. Chem.* **2008**, *51*, 4076–4084; b) K. Robinson, C. J. Easton, A. F. Dulhunty, M. G. Casarotto, *ChemMedChem* **2018**, *13*, 1957–1971.

[21] a) N. L. S. Yue, D. J. Eisler, M. C. Jennings, R. J. Puddephatt, *Inorg. Chem.* **2004**, *43*, 7671–7681; b) N. Yue, Z. Q. Qin, M. C. Jennings, D. J. Eisler, R. J. Puddephatt, *Inorg. Chem. Commun.* **2003**, *6*, 1269–1271; c) N. L. S. Yue, M. C. Jennings, R. J. Puddephatt, *Inorg. Chim. Acta* **2016**, *445*, 37–45.

[22] C. Frassineti, S. Ghelli, P. Gans, A. Sabatini, M. S. Moruzzi, A. Vacca, *Anal. Biochem.* **1995**, *231*, 374–382.

Manuscript received: June 18, 2021
Version of record online: September 6, 2021

